NJC

Accepted Manuscript

This is an *Accepted Manuscript*, which has been through the Royal Society of Chemistry peer review process and has been accepted for publication.

Accepted Manuscripts are published online shortly after acceptance, before technical editing, formatting and proof reading. Using this free service, authors can make their results available to the community, in citable form, before we publish the edited article. We will replace this *Accepted Manuscript* with the edited and formatted *Advance Article* as soon as it is available.

You can find more information about *Accepted Manuscripts* in the Information for Authors.

Please note that technical editing may introduce minor changes to the text and/or graphics, which may alter content. The journal's standard Terms & Conditions and the Ethical guidelines still apply. In no event shall the Royal Society of Chemistry be held responsible for any errors or omissions in this *Accepted Manuscript* or any consequences arising from the use of any information it contains.

ROYAL SOCIETY OF CHEMISTRY

www.rsc.org/njc

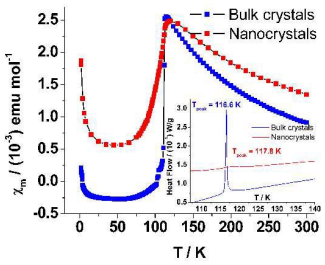

Magnetic, thermal behaviors and phase transition nature are strongly influenced by grain size in one-dimensional S = 1/2 molecular spin systems

Grain size effect on magnetic and phase transition features in one-dimensional S = 1/2 Heisenberg spin chain molecule crystals

Guo-Jun Yuan,[a,b] Yun-Xia Sui,*[c] Jian-Lan Liu[a,b] Xiao-Ming Ren*[a,b,d]

[a] State Key Laboratory of Materials-Oriented Chemical Engineering and College of Science, Nanjing Tech University, Nanjing 210009, P. R. China

[b] College of Materials Science & Engineering, Nanjing Tech University, Nanjing 210009, P. R. China

[c] Centre of Modern Analysis, Nanjing University, Nanjing 210093, P. R. China

[d] State Key Laboratory of Coordination Chemistry, Nanjing University, Nanjing 210093, P. R. China

Tel.: +86 25 58130476

Fax: +86 25 58130481

Email: suiyx@163.com (YXS); xmren@njtech.edu.cn (XMR)

Abstract

In this study, we prepared the sub-micron crystals of one-dimensional (1-D) spin-Peierls-type compounds, 1-(4'-**R**-benzyl)pyridinium-d_5 bis(maleonitriledithiolato)-nickelate (**R** = **Br** or **Cl**), using a facile method, namely, the acetonitrile solution of compound was quickly mixed with excess water (an insoluble solvent). This facile method of preparation gave uniform dispersion of sub-micron crystals with a typical dimension of < 1.0 μm. We observed that the grain size reducing effect the magnetic and phase transition features. With respect to the bulk crystal samples, the powder X-ray diffraction peaks are broadened, the transition temperature T_C is up-shift with $\Delta T_C \approx 1.2$ K for **R** = **Br** vs. 1.0 K for **R** = **Cl**, and the changes of enthalpy and entropy of phase transition are much decreased for the sub-micron crystal samples; In addition, to reduce crystal grain size leads to the onset of strongly Curie-Weiss type paramagnetic background and significant temperature independent paramagnetism.

Keywords: Nickel-bis-dithiolene molecule crystal, spin-Peierls-type transition, sub-microns scale, grain size effect

Introduction

Inorganic crystals, which consist of a network of ordered atoms or ions without discernible molecular unit, generally, show size-dependent electronic properties,[1-3] which is thought to originate from phonon confinement, additional surface phonons, or tensile surface stresses.[4] However, the molecular crystals exhibit usually size-independent electronic properties because molecules are localized entities, the weakly intermolecular interactions extend rarely beyond the nearest neighbors in a typical molecular crystal and make possible the bulk properties of a molecular crystal to regularly be analyzed as the sum of individual molecular contributions, with small perturbations from the intermolecular forces.[5] This is one of main reasons, in the context of molecule crystal, that the study of size-dependent electronic property has received relatively little attention so far. It is possible that the molecular crystals display the size-dependent electronic or magnetic behaviors if there is non-ignorable electron-phonon/spin-phonon interaction.

In previous studies, we designed and achieved a series of 1-D $[Ni(mnt)_2]^-$-based spin-Peierls-type molecule crystals (mnt^{2-} = maleonitriledithiolate),[6] and observed the local structural fluctuation in such magnetic chain systems, which is a typical phenomenon originated from electron-phonon or magnetoelastic coupling interactions.[7] This motivates us to further investigate the magnetic and phase transition natures for such spin-Peierls-type molecule crystals in the nano-scale/sub-micron scale, to gain new evidences of magnetoelastic interaction.

In this paper, the sub-micron crystals of two 1-D $[Ni(mnt)_2]^-$-based spin-Peierls-type compounds, which molecule structure is illustrated in Scheme 1, were prepared using a facile method. The sub-micron crystals of these 1-D spin-Peierls-type transition compounds display some novel natures, such as the critical temperature of spin-Peierls-type transition, T_C, up-shift and the magnetic susceptibility rounded change around T_C with respect to the bulk crystals.

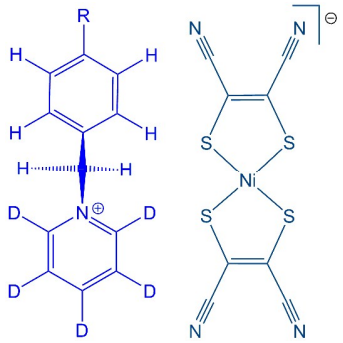

Scheme 1 Molecule structure of 1-(4'-**R**-benzyl)pyridinium-d_5 bis(maleonitriledithiolato)nickelate (**R** = **Br** or **Cl**)

Experimental section

Chemicals and materials

All reagents and chemicals were purchased from commercial sources and used without further purification. The compounds 1-(4'-**R**-benzyl)pyridinium-d_5 bis(maleonitriledithiolato)nickelate (**R = bromo** and **chloro**; abbr. as **Br-1** and **Cl-1**, respectively) and their bulk crystals were obtained by means of the reported approach.[8]

Preparation of sub-micron crystals

400 mL of water, an insoluble solvent, was quickly added to 10 mL of the acetonitrile solution with 595 mg (1.0 mmol) of 1-(4'-bromobenzyl)pyridinium-d_5 bis(maleonitriledithiolato)nickelate, the mixture is vigorously stirred at ambient temperature for 20 min, followed by standing for 10 hours, the precipitate was filtered off using superfine fiber filter membrane and dried under vacuum. The sub-micron crystals were labeled as **Br-2**.

A similar procedure was utilized for the sub-micron crystals preparation of 1-(4'-chlorobenzyl)pyridinium-d_5 bis(maleonitriledithiolato)nickelate and the corresponding sample was labeled as **Cl-2**.

Physical measurements

Power X-ray diffraction (PXRD) data were collected on a Bruker D8 Advance

powder diffractometer operating at 40 kV and 40 mA using Cu Kα radiation with λ = 1.5418 Å. Samples were scanned in the range of 2θ = 5-50° with 0.02°/step and 1.2 s/step. The morphology and crystal grain sizes of the samples were observed using a Hitachi S-3400N Π scanning electron microscopy (SEM) at an operating voltage of 15 KV. Magnetic susceptibility data were measured over the temperature range of 2-300 K using a Quantum Design MPMS-5S superconducting quantum interference device (SQUID) magnetometer. Differential scanning calorimetry (DSC) was carried out on a Q2000 V24.9 Build 121 instrumental in the temperature range of 93-293 K (from -180 to 20 °C) with a rate of 20 $K \cdot min^{-1}$.

Results and discussion

SEM images and PXRD patterns

Figure 1 shows the scanning electron microscopy (SEM) micrographs for **Br-2** and **Cl-2**, respectively, indicating both **Br-2** and **Cl-2** samples to have uniform particle size distribution and the maximum dimensional of particle sizes is about 1.0 μm. It is mentioned that the different batches can give similar size samples using such facile preparation approach (ref. Figure S1).

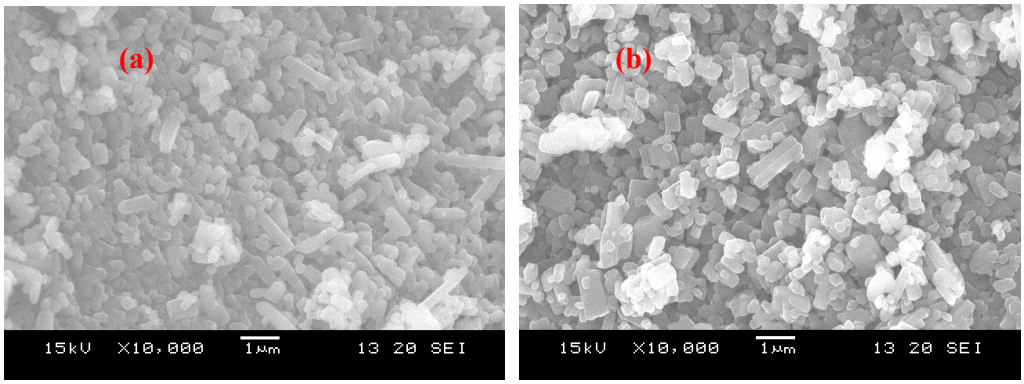

Figure 1 SEM images of (a) **Br-2** (b) **Cl-2**

The powder X-ray diffraction profiles over the 2θ range of 5-50° are shown in Figure 2 and the enlarged ones are displayed in Figure 3. By comparison of the bulk crystals, the broadening effects of diffraction peaks are clearly seen in the diffraction profiles of **Br-2** and **Cl-2** sub-micron crystals owing to the crystal grain size reduced.

The diffraction pattern of the sub-micron crystals **Br-2** is almost the same as its bulk crystals **Br-1**, the peak positions of diffractions, for instance, (1 1 0), (1 3 0), (2 0 0) and (2 2 0) and so on, shift to the lower angle quite little; while these diffraction peaks obviously shift towards the lower angle in the powder X-ray diffraction profile of sub-micron crystals **Cl-2** by comparison of these in the corresponding bulk crystals of **Cl-1**. If the diffraction peaks towards the lower angle is the inherent nature of the sub-micron crystals of **Cl-2**, it means that the lattice expansion occurs in the sub-micron crystals.

It is well-known that the nanocrystals with free surfaces have considerable lattice contraction induced by the large surface/volume ratio,[9] and such a phenomenon is generally observed in metal nanocrystals.[10] In contrast with this common observation, the lattice expansion as the particle size reduced was also found in some metal-oxide nanocrystals.[11,12] Although the exact origin of size-induced the lattice expansion in metal-oxide nanocrystals is still not clearly understood, the structural changes of the species on the nanocrystals surface are thought to play an important role in such a fairly surprising situation, for example, the lattice expansion was observed in the CeO_2 nanocrystals, and the lattice expansion origin of nanocrystals was considered to being due to the valence reduction of metal ions from smaller ion-radii Ce^{4+} to the larger ion-radii Ce^{3+} on the surface of nanocrystals, and the increases of Ce-O bond length on the surface of nanocrystals result in the lattice expansion.[12] For **Cl-1** and **Cl-2**, the PXRD measurements were performed using the crystalline Si powder as an internal standard and shown in Figure S2 in ESI, and the results disclosed that the small difference between the **Cl-1** and **Cl-2** PXRD patterns probably arise from the errors in measurements.

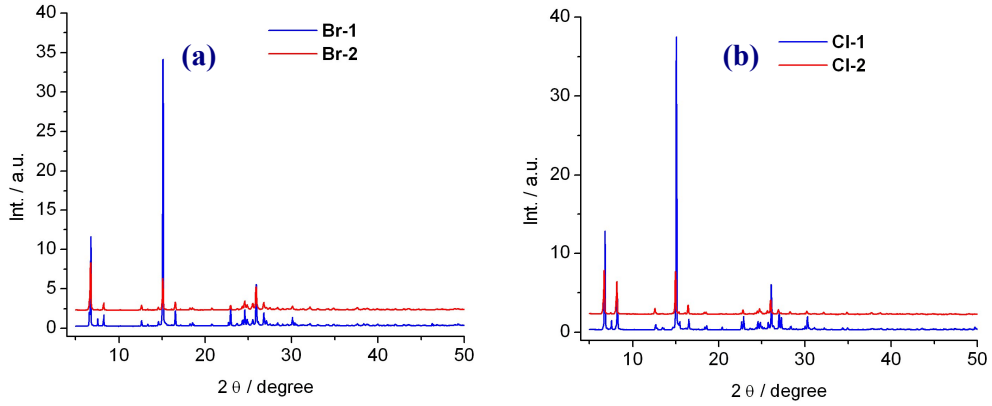

Figure 2 Experimental Powder X-ray diffraction profiles over the 2θ range of 5-50° for (a) **Br-1** and **Br-2** (b) **Cl-1** and **Cl-2**.

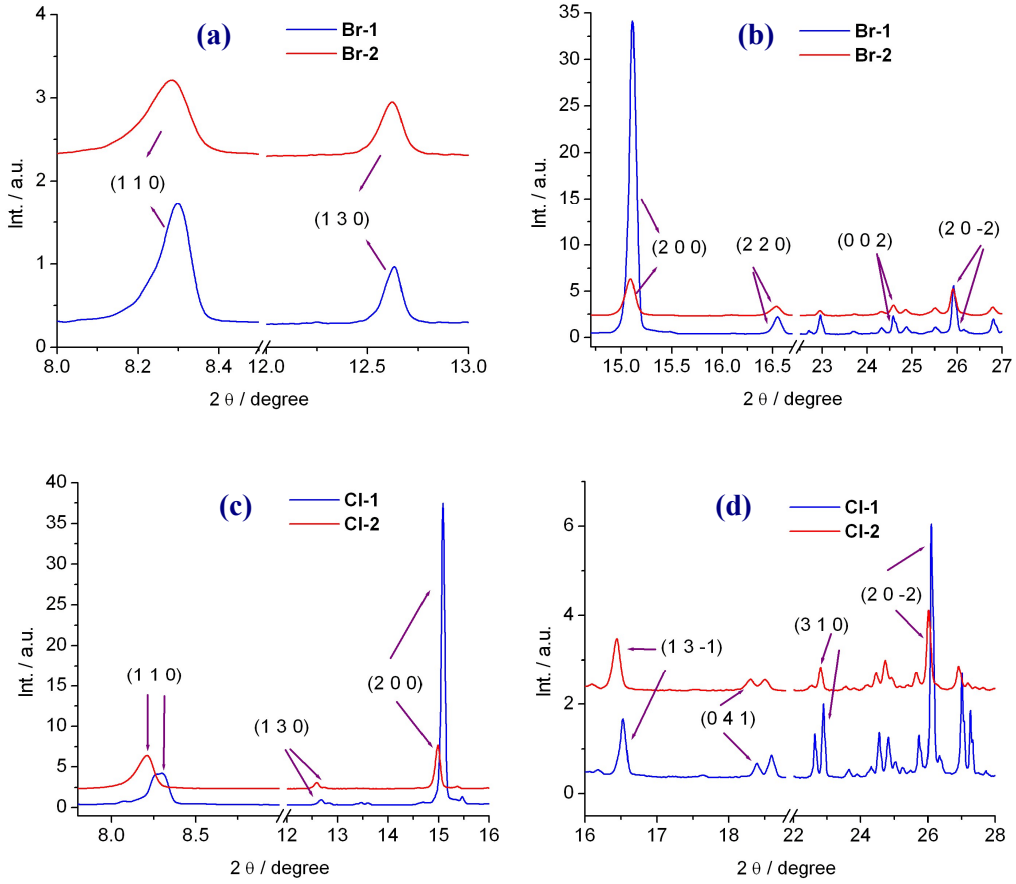

Figure 3 Powdered X-ray diffraction profiles at room temperature for (a, b) **Br-1** and **Br-2** (c, d) **Cl-1** and **Cl-2**.

Magnetic and spin-Peierls-type transition natures

The plots of χ_m-T are displayed in Figure 4a and 4b for **Br-1**, **Br-2**, **Cl-1** and **Cl-2**. The obvious distinctions are observed in the χ_m against T plots between the samples of sub-micron crystals and the corresponding bulk crystals, (1) the magnetic susceptibility change sharply in the bulk crystals, while rounded in the sub-micron crystal sample at the transition. The analogous phenomenon was reported in some spin-crossover (SCO) compounds, where to downscale the particles leads to more gradual magnetic susceptibility change in the thermal SCO process, owing to the particle size dependent cooperative interactions in the lattice of SCO compounds.[13-18] (2) An onset of a strongly paramagnetic background appears in the sub-micron crystals, whereas the diamagnetism (where the negative magnetic susceptibility is clearly seen between 10 and 100 K for **Br-1** and **Cl-1**) occurs in the corresponding bulk crystals below transition temperature. It is easily understandable that to reduce the crystal size induces the strongly Curie-Weiss type paramagnetic background in such 1-D magnetic systems since an antiferromagnetic spin chain of $[Ni(mnt)_2]^-$ is decoupled at the position of the crystal surface, these decoupled $[Ni(mnt)_2]^-$ anions give a contribution to the Curie-Weiss type paramagnetic susceptibility and a larger percentage of the decoupled $[Ni(mnt)_2]^-$ anions are in the surfaces of sub-micron crystals, owing to larger surface/volume ratio, with regard to the bulk crystals.

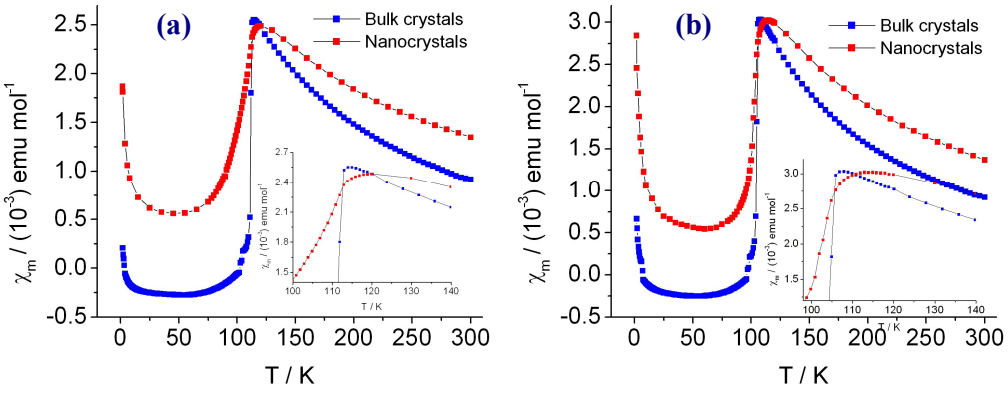

Figure 4 Plots of χ_m-T of (a) **Br-1** and **Br-2** (b) **Cl-1** and **Cl-2** (insets: enlarged plots), respectively.

Given that the spin gap opens below the magnetic transition in a 1-D spin-Peierls

system, the paramagnetic susceptibility contributed from 1-D magnetic chains is ignorable in the lower temperature region owing to the existence of big spin gap, as a result, the Curie-Weiss type paramagnetic background and the temperature independent paramagnetism can be estimated from the fits of temperature-dependent magnetic susceptibilities in the lower temperature region using Eq. (1),

$$\chi_m = \frac{C}{T-\theta} + \chi_o \qquad (1)$$

The first term in Eq.(1) represents the Curie-Weiss type paramagnetic susceptibility; the parameters C and θ correspond to the Curie and Weiss constants, respectively. The parameter χ_0 is the summations of diamagnetism contributed from the atoms core of molecules and the possible van Vleck-type temperature-independent paramagnetic susceptibility originated from the coupling of the ground and excited states through a magnetic field.[19] The fitted parameters of C, θ, χ_0 and the temperature interval used for the fits are summarized in Table 1 for **Br-1**, **Br-2**, **Cl-1** and **Cl-2**, indicating that the amount of only a fraction of 0.3% for **Br-1** versus ~0.7% for **Cl-1** of Curie-Weiss type paramagnetism is estimated in the bulk crystals from the fitted Curie constants, however, the pronounced Curie-Weiss type paramagnetism with a fraction of 1.1% for **Br-2** *versus* 2.1% for **Cl-2** were observed in the sub-micron crystals (ref. Table 1). Another striking feature arose from the particle size reducing is that the temperature-independent paramagnetic susceptibilities appear in the sub-micron crystal samples by comparison of the corresponding bulk crystal samples. For example, the fits of magnetic susceptibility gave the negative χ_0 for the bulk crystals **Br-1** and **Cl-1**, moreover, the χ_0 values are close to the Pascal's constants of the corresponding 1-D spin-Peierls-type compound; however, the positive χ_0 for the sub-micron crystals **Br-2** and **Cl-2**, demonstrating that there exists van Vleck-type temperature independent paramagnetic susceptibility in the sub-micron crystals.

Above the magnetic transition, form the structural viewpoint, the spin-Peierls-type compound shows the magnetic susceptibility character of a Heisenberg uniform antiferromagnetic chain, the corresponding magnetic susceptibility data were further

analyzed using Eq.(2) with Eq.(3),

$$\chi_m = \chi_m(chain) + \frac{C}{T-\theta} + \chi_0 \qquad (2)$$

$$\chi_m(chain) = \frac{Ng^2\mu_B^2}{k_B T} \cdot \frac{A + BX^{-1} + CX^{-2}}{1 + DX^{-1} + EX^{-2} + FX^{-3}} \qquad (3)$$

In Eq.(2), the terms of $C/(T-\theta)$ and χ_0 represent the Curie-Weiss type and temperature-independent magnetic susceptibilities, respectively; the term of χ_m(chain) corresponds to the magnetic susceptibility contributed from the magnetic chains, and the Eq.(3) is deduced from a S = ½ Heisenberg model of uniform chain and is based on the spin Hamiltonian below,

$$\hat{H} = -2J\sum_{i=1}^{n} \hat{S}_{j-1}\hat{S}_j \qquad (4)$$

In Eq.(3), $X = k_BT/|J|$, where J is the magnetic exchange constant of the neighboring spins in a uniform magnetic chain and the coefficients A-F are constants with the values A = 0.25, B = 0.14995, C = 0.30094, D = 1.9862, E = 0.68854, F = 6.0626.[20]

In the fitting procedure, it was supposed that the Curie-Weiss type paramagnetic background and the temperature-independent paramagnetic term, χ_0, are the same in both high- and low-temperature phases for each sample, and these terms were obtained from the fits of magnetic susceptibility data in the low-temperature phase. The fitted magnetic exchange constant J and the temperature interval used for the fits are listed in Table 1. It is mentioned that the fit gave the unreasonable g-factor value besides for **Br-1**, as a result, the g-factor value was fixed in the fitting process. The theoretically reproduced plots of χ_m-T match well with the experimental data for the bulk crystals of both **Br-1** and **Cl-1**, whereas not good for the sub-micron crystals of both **Br-2** and **Cl-2** in the high-temperature phase (ref. Figure S3). The fits of the temperature dependent magnetic susceptibility disclosed that the magnetic exchange constant J within a magnetic chain increases as the crystal particle size reduces in the high temperature phase.

Table 1 the fitted parameters and the used temperature ranges for both sub-micron

crystals and bulk crystals

	Br-1	**Br-2**	**Cl-1**	**Cl-2**
		In low-temperature phase		
C / emu·K·mol^{-1}	1.07(3)×10^{-3}	4.25(6)×10^{-3}	2.61(13)×10^{-3}	8.04(53)×10^{-3}
θ / K	-0.06(6)	-1.16(4)	-0.61(14)	-1.61(22)
χ_0 / emu·mol^{-1}	-2.9(2)×10^{-4}	4.6(4)×10^{-4}	-3.1(7)×10^{-4}	4.0(3)×10^{-4}
Temp. range / K	2-50	2-45	2-50	2-55
		In high-temperature phase		
g	2.02(0)	2.0 (fixed)	2.0 (fixed)	1.9 (fixed)
$\|J\|/k_B$ / K	13.4(4)	36(2)	2.3(1)	11(2)
Temp. range / K	128-300	140-300	124-300	140-300

The phenomenon that crystal grain size effects the phase transition or physical properties of a material has been observed in some ferroelectric or ferromagnetic system. The well-known ferroelectric material $BaTiO_3$ experiences three-step structural phase transitions, namely, the cubic (C) → tetragonal (T) → orthorhombic (O) → rhombohedral (R) transition sequence. Arlt et al.[21] showed that in fine-grained (ca. 1 μm) polycrystalline samples, the O→T transition temperature shifts to higher temperatures with decreasing grain size. In $Sm_{0.5}Sr_{0.5}MnO_3$, Zhou et al.[22] found that all the nanoparticles show a first-order ferromagnetic transition under low magnetic fields, but a second-order one above a critical field HCR. As the particle size decreases, the ferromagnetic transition temperature, the thermal hysteresis width in the magnetizations, and HCR as well as the Weiss constant θ_{PM} in the high-temperature paramagnetic phase exhibit a significant decrease, indicating that the ferromagnetism is weakened and the first-order transition is softened; such a phenomenon is due to the weakened double-exchange interactions and the strongly suppressed charge-ordered antiferromagnetic state by the size reduction, respectively. In our 1-D spin systems, the exact mechanism is not clear for the phenomenon of the crystal grain dependent J at present stage.

Differential scan calorimetry (DSC) measurements were additionally performed to precisely determine the change of T_C for these 1-D spin-Peierls-type systems, and the corresponding curves are shown in Figure 5. The critical temperature of transition, T_C, is upshift with $\Delta T_C \approx 1.2$ K for **Br-2** *versus ca.* 1.0 K for **Cl-2** regarding the bulk

crystal samples.

Theoretically, the expression for spin-Peierls transition temperature, T_C, is of the BCS form

$$k_B T_C = 1.14(pJ)\exp(1/\lambda) \quad (8)$$

$$\lambda = 4g^2 p^2 N_0 / \omega_0^2 \quad (9)$$

$$g = g(\lambda q, q = 2k_f) \quad (10)$$

Where $N_0 = 1/pJ\pi$ is the density of states at k_f for the fermion band, J is the static exchange constant and the only weakly temperature dependent constant p = 1.64 as well as ω_0 and g represent the phonon frequency in the absence of spin interaction and the spin-phonon coupling constant, respectively.[23,24] As a result, the critical temperature of spin-Peierls-type T_C increases with the magnetic coupling interactions (J) within a magnetic chain. In our previous study, such a phenomenon of magnetic exchange constant J dependent T_C was really observed. The T_C in a series of [1-(4'-**R**-benzyl)pyridinium][Pt(mnt)$_2$] salts is much higher than that in the isostructural [1-(4'-**R**-benzyl)pyridinium][Ni(mnt)$_2$] salts with the same substituent R (R = Cl, Br, NO_2, CH_3, $CH{=}CH_2$) owing to the bigger J value in $[Pt(mnt)_2]^-$ salt with respect to the corresponding $[Ni(mnt)_2]^-$ salt.[6a, 6b, 25] Therefore, the fact that the sub-micron crystal samples show higher T_C, with respect to the corresponding bulk crystal samples, is probably related to its J value increase.

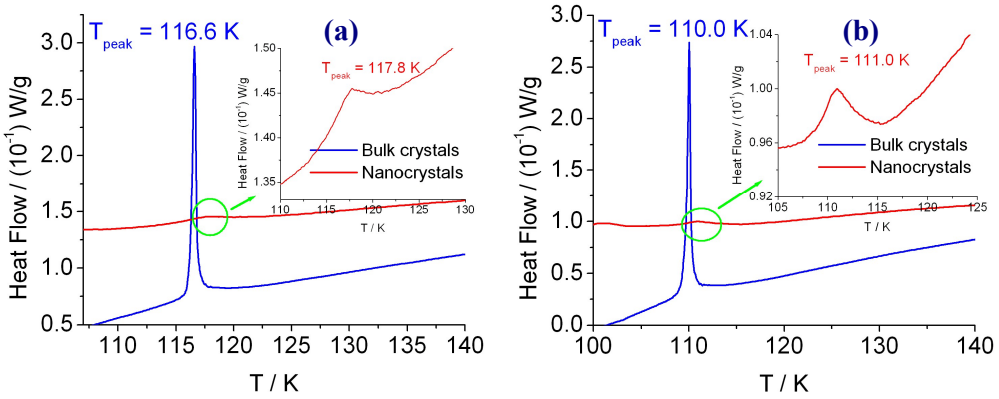

Figure 5 DSC plots of (a) **Br-1** and **Br-2** (b) **Cl-1** and **Cl-2**.

The enthalpies and entropies of the spin-Peierls-type transition, including the contribution of both structure and spin, are estimated as $\Delta H \approx 0.472$ kJ·mol^{-1} and $\Delta S \approx 4.06$ J·K^{-1}·mol^{-1} for **Br-1** *versus* $\Delta H \approx 0.537$ kJ·mol^{-1} and $\Delta S \approx 4.88$ J·K^{-1}·mol^{-1} for **Cl-1**. The transition entropy contributed from the structure is almost equal to zero because the crystal structures are ordered in both the high- and the low-temperature phases. The estimated entropies of phase transition are lower than the theoretical maximum of spin entropies from a mole of S = ½ anions in HT phase to S = 0 anions in LT phase (*Rln2* ≈ 5.76 J·K^{-1}·mol^{-1}),[26] this suggests that a substantial short-range order persists above the magnetic transition temperature of **Br-1** and **Cl-1**. The short-range order is an indication of a lowered dimensionality of the spin system,[27] and is consistent with the uniform chain structure of the $[Ni(mnt)_2]^-$ anions in the crystal **Br-1** and **Cl-1**.[8] The enthalpies and entropies of the spin-Peierls-type transition are estimated as $\Delta H \approx 0.073$ kJ·mol^{-1} and $\Delta S \approx 0.62$ J·K^{-1}·mol^{-1} for **Br-2** *versus* $\Delta H \approx 0.031$ kJ·mol^{-1} and $\Delta S \approx 0.27$ J·K^{-1}·mol^{-1} for **Cl-2**. Obviously, to reduce the crystal grain size gives rise to the enthalpies and entropies of the spin-Peierls-type transition much decreasing. The phenomenon that the enthalpy and entropy of transition reduce with decreasing particle size was also reported in other phase transition material,[28] and the particle size dependent enthalpy and entropy of transition is probably related to the lattice defects, in general, the lattice defect increases with decreasing particle size.

Conclusion and remark

In summary, the sub-micron crystals were prepared for two 1-D $[Ni(mnt)_2]^-$-based spin-Peierls-type compounds. The up-shift of magnetic transition temperature, the onset of a strongly Curie-Weiss type paramagnetic background and the significant temperature independent paramagnetism appear in the sub-micron crystals with respect to the bulk crystals. The strongly Curie-Weiss type paramagnetic background in the sub-micron crystals of two 1-D compounds is due to that an antiferromagnetic spin chain of $[Ni(mnt)_2]^-$ is decoupled at the position of the crystal surface, these decoupled $[Ni(mnt)_2]^-$ anions contribute to the Curie-Weiss type paramagnetic

susceptibility and a larger percentage of the $[Ni(mnt)_2]^-$ anions are on the surfaces of sub-micron crystals with regard to the bulk crystals. In addition, the size-dependent magnetic and phase transition behaviors further support that there exist the phonon confinement effect in 1-D $[Ni(mnt)_2]^-$-based spin-Peierls-type compounds.

Acknowledgement

Authors thank the Priority Academic Program Development of Jiangsu Higher Education Institutions, Special Research Found for the Doctoral Program of Higher Education and National Nature Science Foundation of China for financial support (grant no. 20123221110013 and 21271103).

Supporting materials

The theoretical reproduced and experimental χ_m-T plots and the SEM images of **Br-2**, **Cl-2** prepared in different batch are included in ESI.

References

1. (a) J. S. Biteen, N. S. Lewis, H. A. Atwater, A. Polman, *Appl. Phys. Lett.* **2004**, 84, 5389; (b) Y. F. Li, A. J. Mao, Y. Li, X. Y. Kuang, *J. Mol. Model.* **2012**, 18, 3061.
2. (a) V. Luca, *J. Phys. Chem. C* **2009**, 113, 6367; (b) S. K. Sahoo, S. Pal, P. Sarkar, C. Majumder, *Chem. Phys. Lett.* **2011**, 516, 68; (c) A. B. Moshe, D. Szwarcman, G. Markovich, *ACS Nano* **2011**, 5, 9034; (d) B. Wei, K. Zheng, Y. Ji, Y. F. Zhang, Z. Zhang, X. D. Han, *Nano Lett.* **2012**, 12, 4595.
3. (a) C. B. Murray, D. J. Norris, M. G. Bawendi, *J. Am. Chem. Soc.* **1993**,115, 8706; (b) A. P. Alivisatos, *Science* **1996**, 271, 933; (c) H. Zeng, J. Li, J. P. Liu, Z. L. Wang, S. Sun, *Nature* **2002**, 420, 395.
4. G. S. Li, J. Boerio-Goates, B. F. Woodfield, L. P. Li, *Appl. Phys. Lett.* **2004**, 85, 2059.
5. Y. Wang, N. Herron, *J. Phys. Chem.* **1991**, 95, 525.
6. (a) X. M. Ren, Q. J. Meng, Y. Song, C. S. Lu, C. J. Hu, X. Y. Chen, *Inorg. Chem.* **2002**, 41, 5686; (b) Z. F. Tian, H. B. Duan, X. M. Ren, C. S. Lu, Y. Z. Li, Y. Song, H. Z. Zhu, Q. J. Meng, *J. Phys. Chem. B* **2009**, 113, 8278; (c) H. B. Duan, X. M. Ren, Q. J. Meng, *Coord. Chem. Rev.* **2010**, 254, 1509.
7. (a) X. M. Ren, T. Akutagawa, S. Noro, S. Nishihara, T. Nakamura, Y. Yoshida, K. Inoue, *J. Phys. Chem. B* **2006**, 110, 7671; (b) X. M. Ren, S. Nishihara, T. Akutagawa, S. Noro, T. Nakamura, W. Fujita, K. Awaga, Z. P. Ni, J. L. Xie, Q. J. Meng, R. K. Kremer, Dalton Trans. **2006**, 1988.
8. G. J. Yuan, S. P. Zhao, C. Wang, X. M. Ren, J. L. Liu, *Chem Commun.* **2011**, 47, 9489.
9. (a) C. W. Mays, J. S. Vermaak, D. Kuhlmann-Wilsdorf, *Surf. Sci.* **1968**, 12, 134; (b) H. J. Wasserman, J. S. Vermaak, *Surf. Sci.* **1972**, 32, 168; (c) G. Apai, J. F. Hamilton, *Phys. Rev. Lett.* **1979**, 43, 165; (d) Q. Jiang, L. H. Liang, D. S. Zhao, *J. Phys. Chem. B*, **2001**, 105, 6275.
10. A. Taneda, Y. Kawazoe, *J. Magn. Soc. Jpn.* **1999**, 23, 679.
11. V. R. Palkar, P. Ayyub, S. Chattopadhyay, and M. Multani, *Phys. Rev. B* **1996**, 53,

2167.

12. S. Tsunekawa, K. Ishikawa, Z. Q. Li, Y. Kawazoe, and A. Kasuya, *Phys. Rev. Lett.* **2000**, 85, 3440.
13. I. Yu. Barskaya, E. V. Tretyakov, R. Z. Sagdeev, V. I. Ovcharenko, E. G. Bagryanskaya, K. Yu. Maryunina, T. Takui, K. Sato, .M. V. Fedin, *J. Am. Chem. Soc.* **2014**, 136, 10132.
14. P. Durand, S. Pillet, E.-E. Bendeif, C. Carteret, M. Bouazaoui, H. E. Hamzaoui, B. Capoen, L. Salmon, S. Hebert, J. Ghanbaja, L. Arandah, D, Schaniel, *J. Mater. Chem. C*, **2013**, 1, 1933.
15. *Spin-Crossover Materials: Properties and Applications;* M. A. Halcrow Ed.; John Wiley & Sons: Chichester, UK, **2013**.
16. P. Gütlich, H. A. Goodwin, *Top. Curr. Chem.* **2004**, 233.
17. A. Bousseksou, G. Molnar, L. Salmon, W. Nicolazzi, *Chem. Soc. Rev.* **2011**, 40, 3313.
18. J. Larionova, L. Salmon, Y. Guari, A. Tokarev, K. Molvinger, G. Molnar, A. Bousseksou, *Angew. Chem., Int. Ed.* **2008**, 47, 8236.
19. van Vleck, J. H. *The Theory of Electric and Magnetic Susceptibilities*, Oxford, London, **1932**.
20. (a) J. C. Bonner, M. E. Fisher, *Phys. Rev. A* **1964**, 135 (3A), A640; (b) W. E. Hatfild, *J. Appl. Phys.* **1981**, 52, 1985.
21. G. Arlt, D. Hennings, G. de With, *J. Appl. Phys.* 1985, **58**, 1619.
22. S. M. Zhou,Y. Q. Guo, J. Y. Zhao, C. L. Wang, L. F. He, L. Shi, *J. Appl. Phys.* 2012, **111**, 056104.
23. R. K. Kremer, R. W. Henn, A. Faißt, J. Wosnitza, H. v. Löhneysen, *Czech. J. Phys.*, 1996, **46**, 1977.
24. E. Pytte, *Phys. Rev. B* 1974, **10**, 4637.
25. (a) X. M. Ren, H. Okudera, R. K. Kremer, Y. Song, C. He, Q. J. Meng, P. H. Wu, *Inorg. Chem.* 2004, **43**, 2569; (b) D. B. Dang, C. L. Ni, Y. Bai, Z. F. Tian, Z. P. Ni, L. L. Wen, Q. J. Meng, S. Gao, *Chem. Lett.* 2005, **34**, 680; (c) W. H. Ning, X. R. Chen, J. L. Liu, H. Yang, X. M. Ren, *Dalton Trans.* 2014, **43**, 2997; (d) W. H.

Ning, L. Zhai, X. M. Ren, *Synth. Met.* 2015, **199**, 255.

26. X. M. Ren, T. Akutagawa, S. Nishihara, T. Nakamura, W. Fujita, K. Awaga, *J. Phys. Chem. B* 2005, **109**, 16610.
27. S. N. Bhatia, C. J. O'Connor, R. L. Carlin, H. A. Algra, L. J. DeJongh, *Chem. Phys. Lett.* 1977, **50**, 353.
28. M. J. M. Van Oort, M. L. Cotton, *Thermochim. Acta* 1993, **219**, 245.